Stanford Exploration Project, Report 72, December 18, 1997, pages 1–220

Stanford Exploration Project, Report 72, December 18, 1997, pages 1–220

A simple wavefield separation scheme

Dave Nichols[1]

keywords: *velocity, approximation, elastic, near surface*

ABSTRACT

Exact separation of the different wavetypes in a multicomponent dataset requires knowledge of all the elastic properties of the near surface. I propose an approximate scheme that uses a small number of "separation parameters." The approximate scheme uses a three stage approach; at each stage a maximum of three parameters must be estimated. I demonstrate the effectiveness of this scheme on a synthetic dataset.

INTRODUCTION

In an earlier paper (Nichols, 1989) I proposed a method for separating the different wavetypes in a nine-component seismic dataset. My method is an approximate method that does not rely on knowledge of the elastic properties of the near surface. This contrasts with exact separation methods, such as that proposed by Herrmann et al. (1989), which require knowledge of the near surface properties.

In this paper I review the method that I presented in my previous paper. I use a first order approximation of the exact slowness dependent separation operators. I show that this approximation is valid for the range of slownesses acquired in a typical surface seismic experiment. The separation algorithm involves the estimation of several separation parameters. I discuss several methods of estimating these parameters and apply the separation scheme to a very simple synthetic seismic dataset.

WAVEFIELD DECOMPOSITION

In a nine-component seismic, survey sources and receivers are oriented along each of the three coordinate axes. The experiment is recorded for every combination of source and receiver orientation. The recorded wavefield may be represented as a

[1]**email:** not available

matrix of data; the rows correspond to the direction of the source and the columns to the direction of the receiver. Each element of the matrix is one shot record.

$$P_{raw}(\mathbf{r},t) \equiv \begin{pmatrix} Xx(\mathbf{r},t) & Xy(\mathbf{r},t) & Xz(\mathbf{r},t) \\ Yx(\mathbf{r},t) & Yy(\mathbf{r},t) & Yz(\mathbf{r},t) \\ Zx(\mathbf{r},t) & Zy(\mathbf{r},t) & Zz(\mathbf{r},t) \end{pmatrix}$$

The nine-components that we wish to process are those that correspond to downgoing waves of one wavetype at the source and upcoming waves of one wavetype at the receiver. We can represent this data as a new matrix where the rows correspond to the downgoing wavetype at the source and the columns correspond to the upcoming wavetype at the receiver.

$$P_{decomposed}(\mathbf{r},t) \equiv \begin{pmatrix} S_1s_1(\mathbf{r},t) & S_1s_2(\mathbf{r},t) & S_1p(\mathbf{r},t) \\ S_2s_1(\mathbf{r},t) & S_2s_2(\mathbf{r},t) & S_2p(\mathbf{r},t) \\ Ps_1(\mathbf{r},t) & Ps_2(\mathbf{r},t) & Pp(\mathbf{r},t) \end{pmatrix}$$

The transformation from the recorded wavefield to the desired wavefield takes the form of linear operators that are applied for both source and receiver coordinates.

$$P_{decomposed} = A_{source}\ P_{raw}\ A^T_{receiver}$$

As many authors have noted, this transformation is best performed in the $(\mathbf{k},\omega)$ domain or the $(\mathbf{p},\tau)$ domain as the operators are functions of the horizontal slowness. I choose to perform the decomposition in the $(\mathbf{p},\tau)$ domain so that I can use a trace-by-trace method rather than a sample-by-sample method.

Operator symmetries

For orthorhombic media with a horizontal plane of symmetry there are certain symmetries to the operator. The elements of the operator will be either symmetric or anti-symmetric functions of the slowness:

$$\begin{bmatrix} \text{Symm} & \text{Symm} & \text{Anti} \\ \text{Symm} & \text{Symm} & \text{Anti} \\ \text{Anti} & \text{Anti} & \text{Symm} \end{bmatrix}.$$

The exact linear operator has elements that can be expressed as polynomial functions of the horizontal slowness. By truncating the operator to low order in slowness I obtain an approximate operator that is valid for small angles of propagation (Nichols, 1989).

The zeroth order operator

The zeroth order operator has the form

$$\begin{bmatrix} \cos(\phi)/2 & \sin(\phi)/2 & 0 \\ -\sin(\phi)/2 & \cos(\phi)/2 & 0 \\ 0 & 0 & 1/2 \end{bmatrix}.$$

This is the familiar source and receiver rotation operator described by Alford(1986).

The first order operator

The approximate operator with elements that are first order polynomials in the slowness has four new elements, these are anti-symmetric terms in the operator:

$$\begin{bmatrix} \cos(\phi)/2 & \sin(\phi)/2 & a_1 p_x + b_1 p_y \\ -\sin(\phi)/2 & \cos(\phi)/2 & a_2 p_x + b_2 p_y \\ a_3 p_x + b_3 p_y & a_4 p_x + b_4 p_y & 1/2 \end{bmatrix}.$$

A step-by-step separation scheme

The first order operator can be further approximated as a cascade of three operators.

$$A3 = \begin{bmatrix} 1 & 0 & 0 \\ 0 & 1 & y_{23} \cdot p_y \\ 0 & y_{32} \cdot p_y & 1 \end{bmatrix}$$

pre-multiplying,

$$A2 = \begin{bmatrix} 1 & 0 & x_{13} \cdot p_x \\ 0 & 1 & 0 \\ x_{31} \cdot p_x & 0 & 1 \end{bmatrix}$$

pre-multiplying,

$$A1 = \begin{bmatrix} \cos(\phi)/2 & \sin(\phi)/2 & 0 \\ -\sin(\phi)/2 & \cos(\phi)/2 & 0 \\ 0 & 0 & 1/2 \end{bmatrix}$$

$$P_{decomposed} = A3\,A2\,A1\;P_{raw}\;A1^T\;a2^T\;A3^T$$

The separation procedure has three stages.

$A1$ A rotation about the z-axis to separate the two S-wavetypes.

$A2$ An operator to separate P from S_1. This operator has two free parameters that need to be estimated.

$A3$ An operator to separate P from S_2. This operator also has two free parameters that need to be estimated.

VALIDITY OF THE FIRST ORDER APPROXIMATION

To examine the validity of the approximation I numerically calculated the exact operators for an orthorhombic medium. The elastic constants for this medium were generated by calculating the elastic constants for a layered medium with plane-vertical cracks at 20° to the x-axis. Each graph in the grid of figure **??** is a plot of the amplitude of one element of the 3×3 separation operator as a function of slowness. If the first order approximation is exactly valid the symmetric elements would be horizontal lines and the anti-symmetric elements would be lines with constant slope. Clearly, the first order approximation is not exact. However it is a reasonable approximation for a range of slownesses around zero.

Figure **??** shows the exact operator after a coordinate frame rotation of 20° has been applied. This operator should be the combination of the second and third stages of the separation process. Note that the scaling by 0.5 has not been accounted for in this transformation. If the first order approximation and the separation of the rotation operator were exact we would expect to see a flat line at 0.5 for each of the symmetric elements and a straight line passing through (0.,0.) for the anti-symmetric elements. Again the first order approximation is good for a reasonable range of slownesses. The slownesses are expressed in sec./km. The first order approximation appears to be reasonable for slowness values up to 0.15, which for this medium corresponds to a P-wave propagating at 45 degrees to the vertical and an S-wave propagating at 25 degrees to the vertical. This are both large angles for typical surface seismic experiments. I consider the first order approximation to be a reasonable one for this set of elastic constants. Whether it is always a good approximation is a topic that needs further study.

ESTIMATION OF SEPARATION PARAMETERS

At each stage of the separation process there are one or two parameters that must be estimated. If the full elastic properties of the near surface were known the parameters

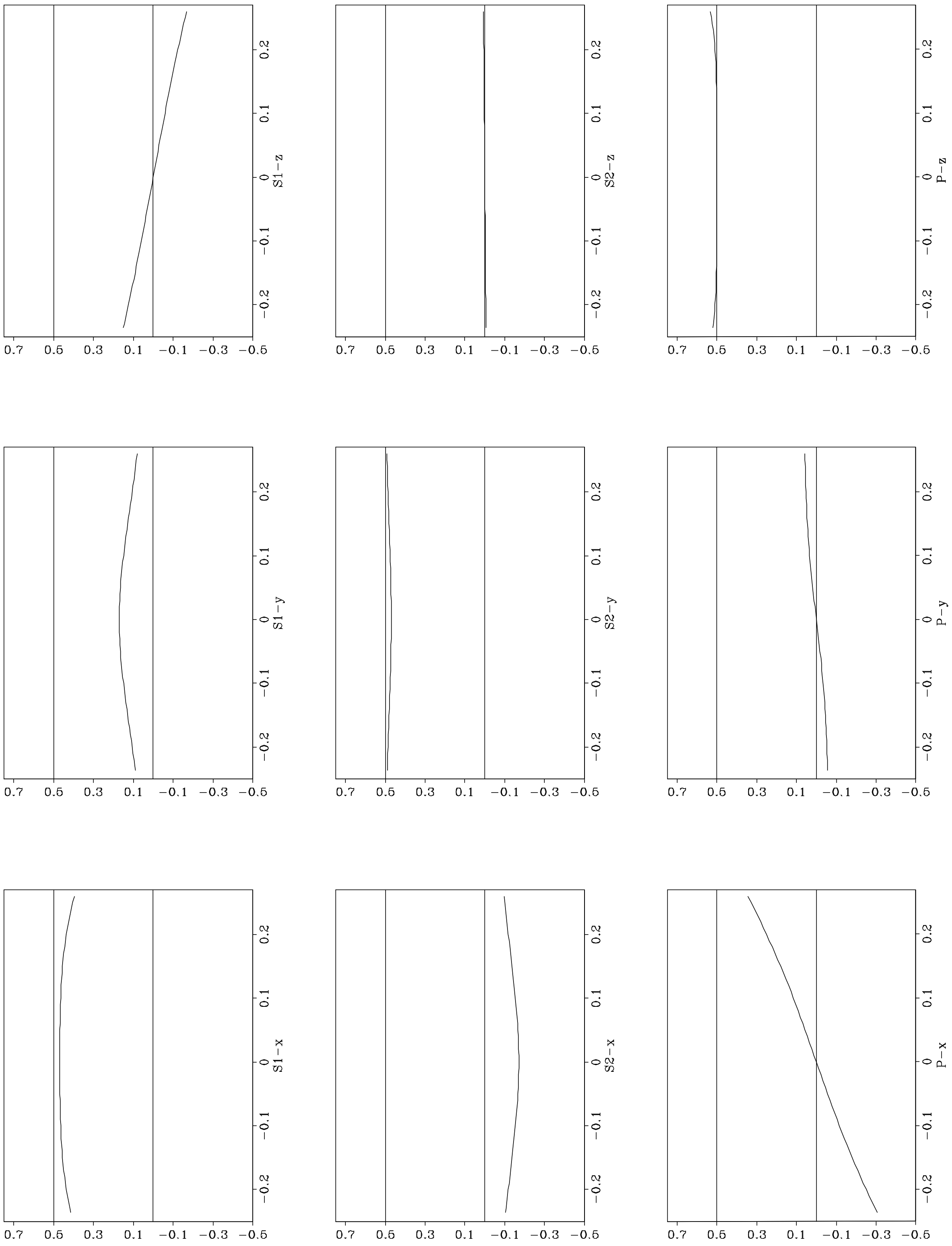

Figure 1: Exact separation operator for a rotated orthorhombic medium. Each element of the operator is plotted as a function of slowness. dave-exact-oper [ER]

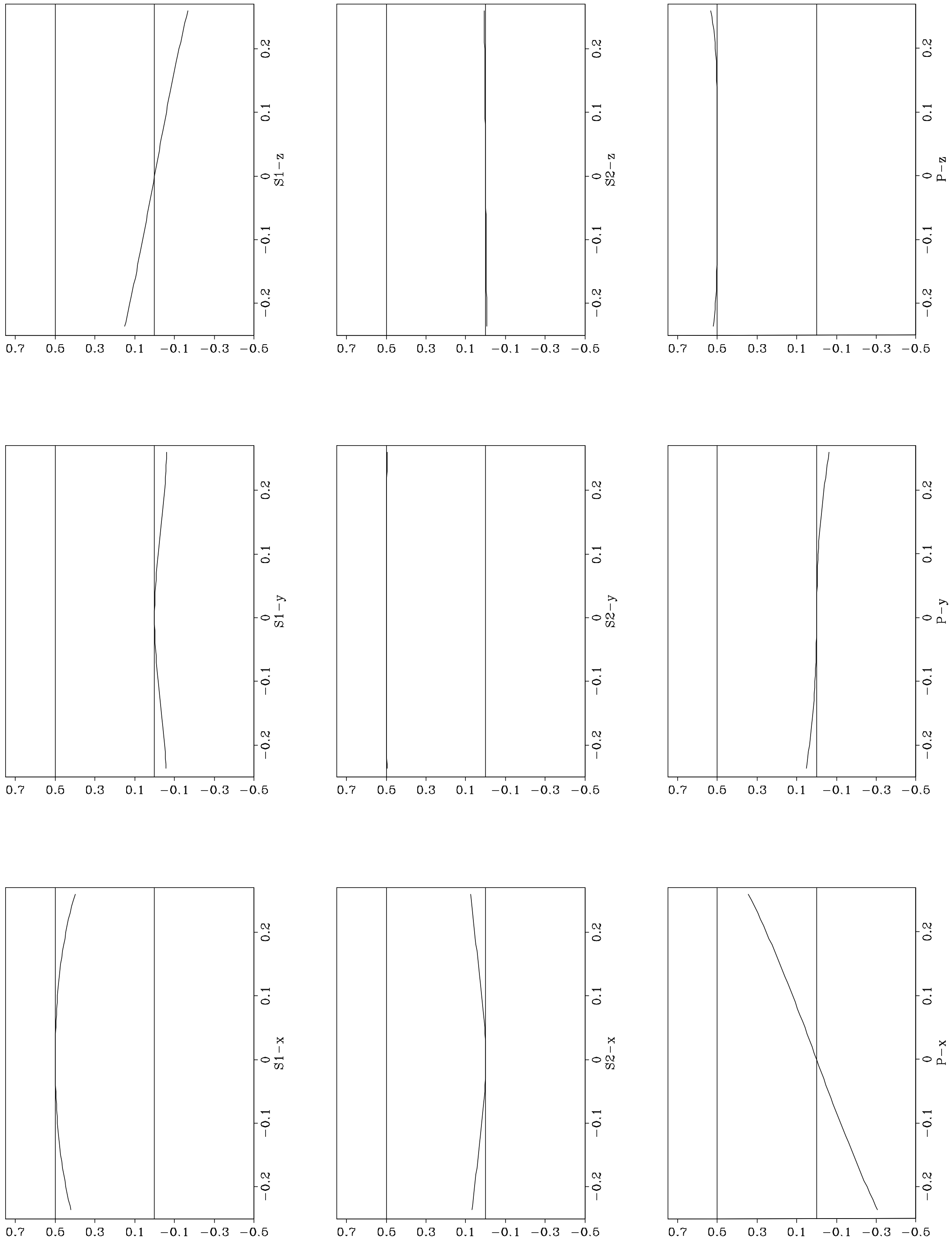

Figure 2: Exact separation operator with the rotation component removed. Each element of the operator is plotted as a function of slowness. $\boxed{\text{dave-rot-exact}}$ [ER]

could be calculated. In a practical processing scheme these parameters must be estimated from the recorded data. We require an objective function that is a measure of the effectiveness of the wavefield separation at each step.

S-wave separation

Since the amplitude of converted S-S waves (S_1-S_2 or S_2-S_1) is usually low we can use total energy in the X'-y' and Y'-x' sections (the horizontal components on the rotated coordinate frame) as a measure of the separation. This is the method that Alford(1986) introduced; the reference frame of the source and receiver components is rotated until the energy in the converted S-S wave sections is minimized. The estimation can be performed on shot gathers or on CMP-stacked data. If shot gathers are used the estimation can be contaminated by noise and unwanted wavetypes (e.g. S-P waves) in the horizontal component shot gathers. By stacking with a suitable S-wave velocity function the S-wave signals are chosen in preference to other arrivals. After suitable rotation angles have been estimated using the stacked data, the rotation can be applied to the shot gathers in preparation for the next stage of the separation algorithm, the P-S wave separation.

P-S wave separation

To estimate the P-S separation coefficients I use a different type of objective function. The energy in the P-s and S-p panels is not a suitable measure because we expect to observe converted waves with significant amplitudes.

A human looking at a gather containing P and S waves often uses the moveout of the events to discriminate between then. With this in mind I have chosen to use an objective function that is calculated in constant velocity stack space. If a section contains only upcoming P waves we would expect to see significant amplitudes at P-p and S-p velocities but none at S-s velocities. A section containing only upcoming S-waves should only have energy at S-s and P-s velocities.

To use this separation procedure a set of velocity “corridors” must be defined. These corridors define the regions in time/velocity space in which the different event types are expected to occur.

There are several possible objective functions that can be used to estimate the best separation parameters.

- F1 = Minimize energy in “wrong” part of velocity space.
- F2 = Minimize the ratio of energy on “wrong” part of velocity space to energy in “right” part of velocity space.
- F3 = Minimize the cross correlation of the S-S and P-P velocity panels within the P-P and S-S corridors.

Calculation of the P-S separation objective function

One way to calculate the objective function is to take the $p - \tau$ data, apply a separation operator, calculate a set of constant velocity stacks, and finally calculate the objective function in velocity stack space. If a repeated calculation of the objective function is required this would appear to be prohibitively expensive since each calculation involves a set of constant velocity stacks. However this cost can be overcome by reordering the operations. The idea is illustrated in figure **??** . The wavefield separation and the velocity stack are both linear operators. These operators can be reordered so that only one velocity stack step is necessary. A weighted combination of the velocity stacks can be used to calculate a velocity stack for the separated data.

The calculation of the objective functions is relatively simple. For example consider the receiver separation operator for the P-S_1 wavetypes. The original data is Xx, Xz, Zx, and Zz data in the $p - \tau$ domain. The following velocity panels are calculated, $V(Xx)$, $V(pXz)$, $V(pZx)$, $V(Zz)$. We can then calculate the velocity panels for the separated data by taking a linear combination of these panels.

$$
\begin{aligned}
V(Xs_1) &= V(Xx) + \alpha V(pXz) \\
V(Zp) &= V(Zz) + \beta V(pZx)
\end{aligned}
$$

I define the cross-energy operators for the Pp and Ss corridors in velocity spaceas

$$
\begin{aligned}
< A, B >_{Pp} &= \Sigma_{i,j \in Pp} A(i,j) B(i,j) \\
< A, B >_{Ss} &= \Sigma_{i,j \in Ss} A(i,j) B(i,j)
\end{aligned}
$$

The three proposed objective functions can then be written as,

$$
\begin{aligned}
F1 &= < V(Xs_1), V(Xs_1) >_{Pp} + < V(Zp), V(Zp) >_{Ss} \\
F2 &= \frac{< V(Xs_1), V(Xs_1) >_{Pp} + < V(Zp), V(Zp) >_{Ss}}{< V(Xs_1), V(Xs_1) >_{Ss} + < V(Zp), V(Zp) >_{Pp}} \\
F3 &= < V(Xs_1), V(Zp) >_{Pp} + < V(Xs_1), V(Zp) >_{Ss} .
\end{aligned}
$$

On substituting the expressions for the separated velocity panels and minimizing by setting $\partial \alpha = 0$ and $\partial F / \partial \beta = 0$, I obtain explicit expressions for α and β from the F1 and F3 objective functions. The F2 objective function does not produce such a simple result but a scan of possible parameters is a relatively cheap operation:

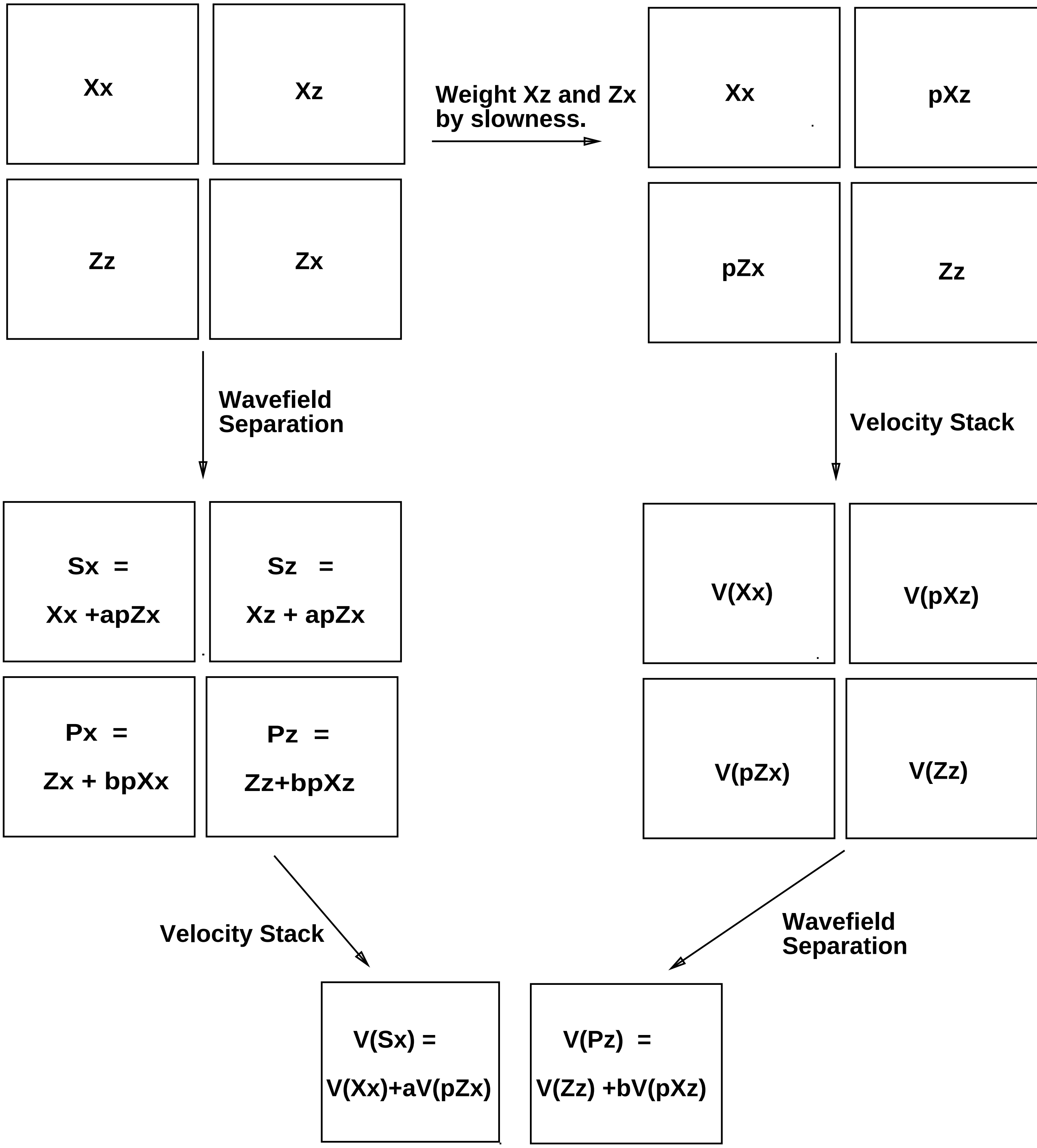

Figure 3: Equivalent methods of calculating the velocity spectra of data separated with different operators. dave-flowdiag [NR]

F1

$$\alpha = \frac{-2 < V(Xx), V(pXz) >_{Pp}}{< V(pXz), V(pXz) >_{Pp}}$$
$$\beta = \frac{-2 < V(Zz), V(pZx) >_{Ss}}{< V(pZx), V(pZx) >_{Ss}}$$

F3

$$\alpha = \frac{- < V(pZx), V(Xx) >_{Pp+Ss}}{< V(pXz), V(pZx) >_{Pp+Ss}}$$
$$\beta = \frac{- < V(pXz), V(Zz) >_{Pp+Ss}}{< V(pXz), V(pZx) >_{Pp+Ss}} .$$

SYNTHETIC DATA EXAMPLES

I modeled the response of a simple one layered model to a unit displacement source on the free surface. The surface layer is the orthorhombic medium used in my earlier examples. The modeling algorithm is the phase shift scheme I described in an earlier report (Nichols, 1991). A synthetic nine-component gather is shown in Figure **??**. It is displayed in the $\tau - p$ domain. The X-x section clearly has many different wavetypes present in the gather. The first event is the P-p wave the second is the P-s and S-p arrivals. The last two events are the two S-s wave arrivals. The two shear waves are split even at zero slowness because this is an orthorhombic medium.

Source and receiver rotation by 20° gives the gather shown in Figure **??**. The horizontal component sections have been diagonalized at zero slowness where the rotation is the exact operator for S-wave separation. The two shear waves have been reasonably separated at all but the highest slownesses. However the horizontal component sections in the rotated reference frame still contain P-p energy and converted wave energy.

Figure **??** shows the constant velocity stack panels for the X-x and Z-z components of the data. There is coherent energy at three separate places on the panel. These correspond to the different reflection events, P-P, P-s/S-p and S-s.

The next stage of the separation process is to estimate the P/S_1 separation coefficients for the receiver operator. Figure **??** is a contour plot of the "F2" objective function for a range of separation coefficients. The values of the coefficients at the minimum of this plot were used in a receiver separation operator that was applied to the synthetic data. The resulting gather is displayed in Figure **??**. The first column of this plot should now correspond to an "S_1" receiver. Therefore there should be no upcoming P-waves visible on the first column. Similarly the last column should now correspond to a "P-receiver" there are no upcoming S-waves visible in this column. S-p waves are still visible in the bottom right section because the Z source generates both P- and S-waves. Figure **??** shows the constant velocity stacks after receiver

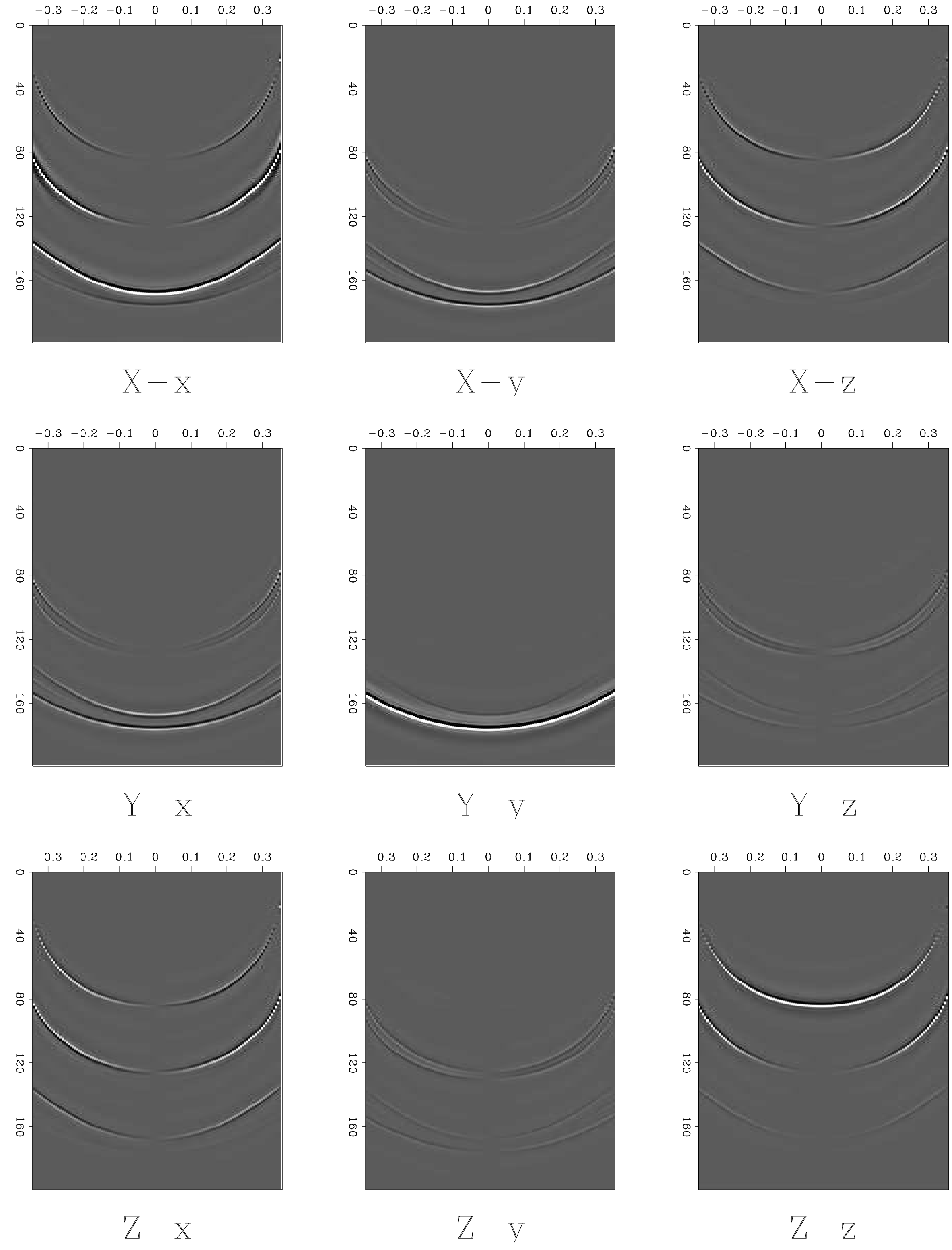

Figure 4: Synthetic nine-component shot gather shown in the $\tau - p$ domain. Many different wavetypes can be seen on each component. dave-orig [ER]

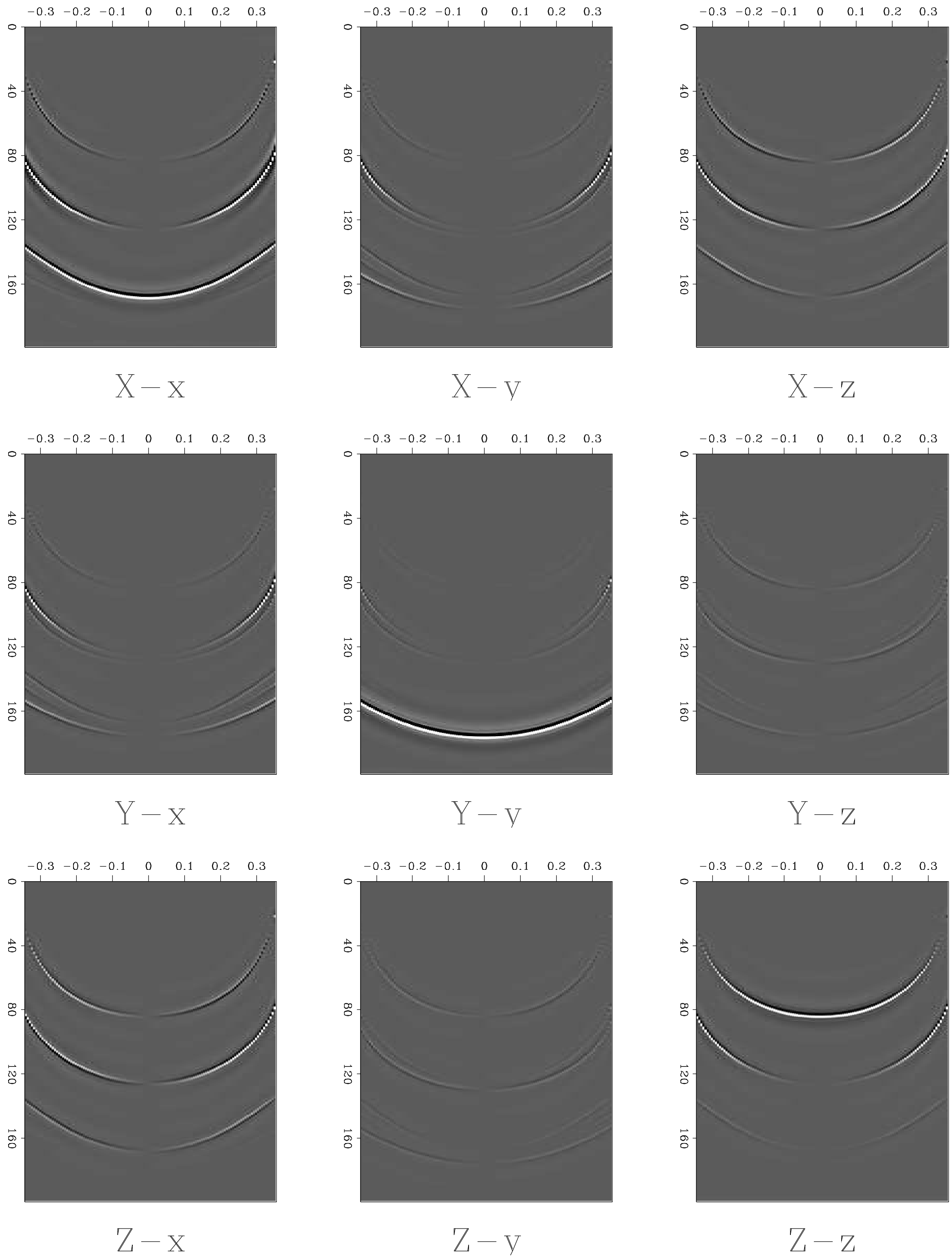

Figure 5: Nine component gather after source and receiver rotation by 20°. The two shear wavetypes have been totally separated at zero slowness and approximately separated at other slownesses. dave-rotated [ER]

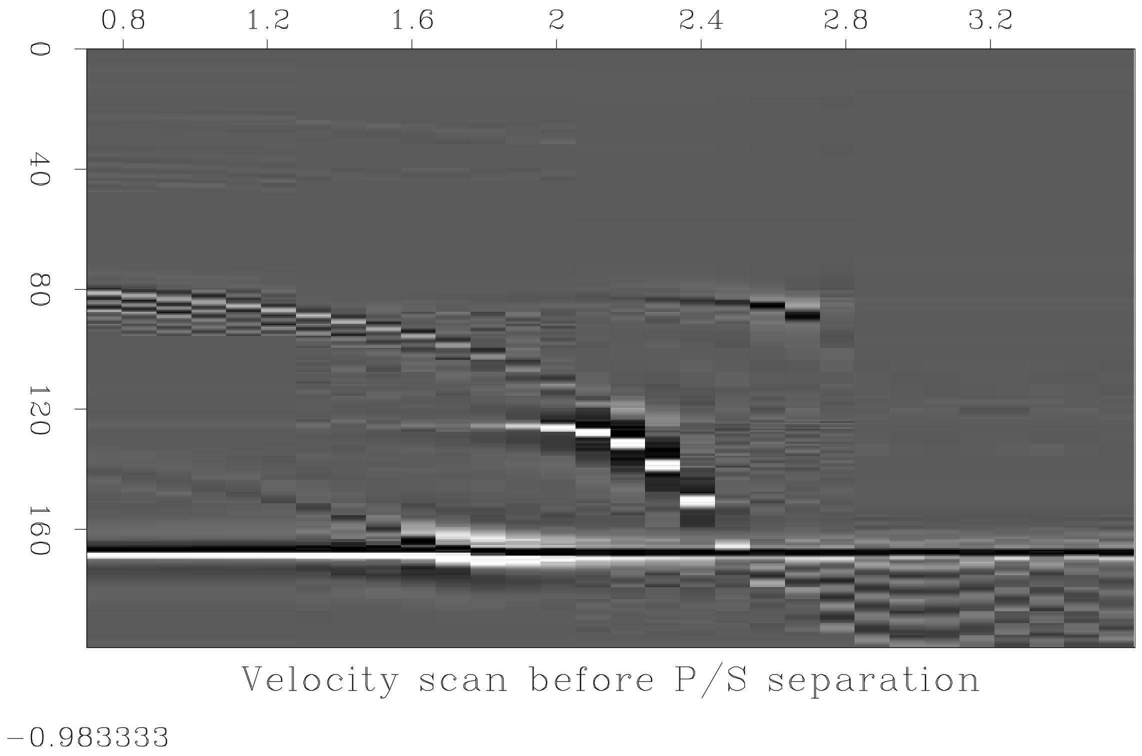

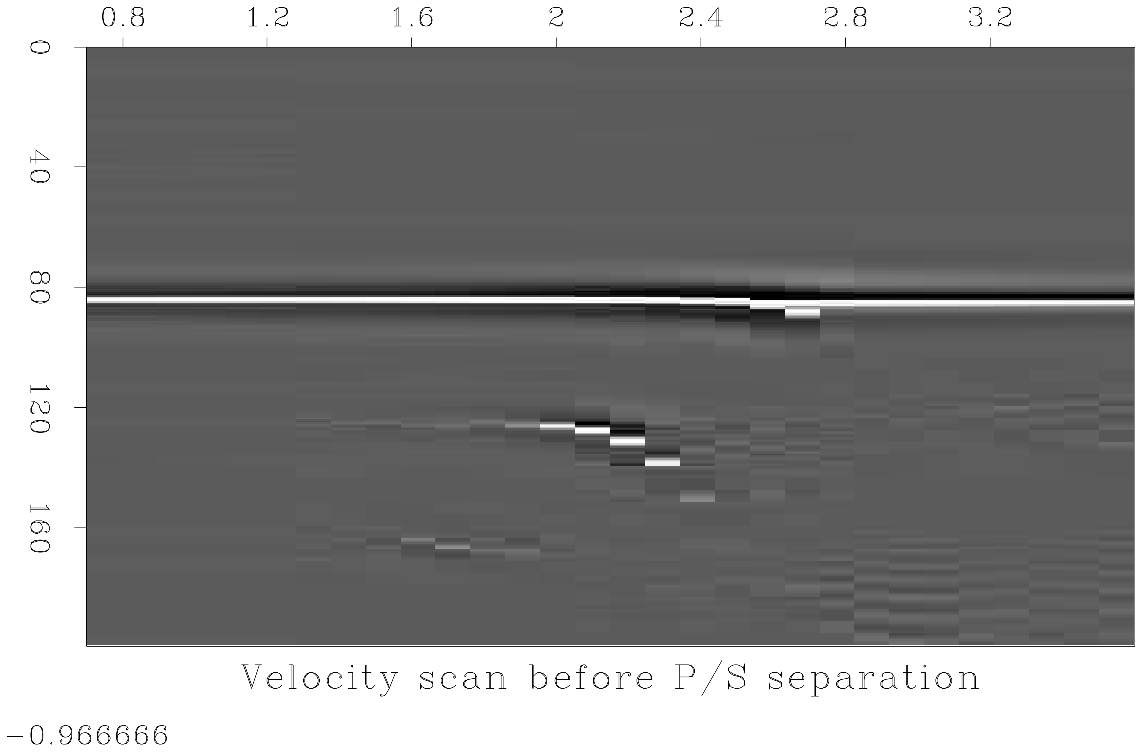

Figure 6: Constant velocity stack panels for the rotated data. The top panel is the X-x component and the bottom panel is the Z-z component. dave-vel-rot [ER]

separation. There is almost no energy at the S-s wave velocity on the Z-p velocity panel and no energy at the P-p wave velocity on the X-s_1 velocity panel.

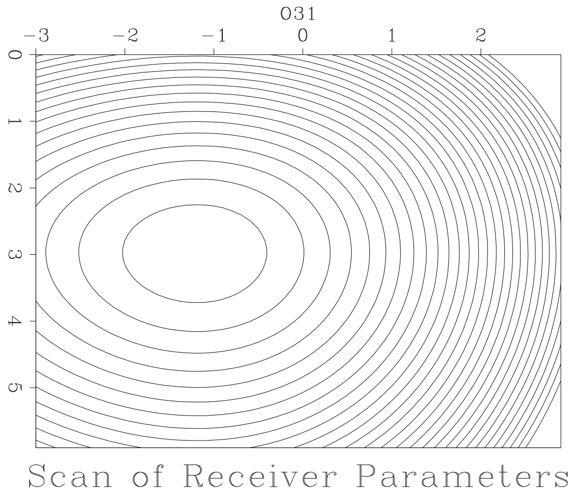

Figure 7: Contour plot of the F2 objective function for the receiver separation parameters. dave-rec-obj [ER]

A similar P/S_1 separation operator was estimated for the source operator and applied to the data. The result is shown in Figure **??**. Although the separation is not complete at the highest slownesses the P- and S_1-waves have been completely separated for a wide range of slownesses around zero slowness. In particular the separation of the two converted wavetypes has been particularly successful, compare the original data in Figure **??** with the final separation result in Figure **??**. The regions where the separation is unsuccessful correspond the to regions in which the first order approximation breaks down. In this example I have not yet applied the final stage of the process, the P/S_2 wave separation.

CONCLUSIONS

By decomposing the exact operator into three approximate operators I have broken the wavefield separation problem into three steps. At each step I must estimate at most two parameters to find those that best separate the different wavetypes. At no point do I attempt to find the full set of elastic constants for the near surface, I only estimate separation parameters. The approximation of the operator is valid over a wide enough range of slowness to be a useful wavefield decomposition process. The great virtue of this method is its simplicity. It is only slightly more complicated than the simple source and receiver rotation but it successfully addresses the problem of separating P-waves and S-waves in anisotropic media.

REFERENCES

Alford, R., 1986, Shear data in the presence of azimuthal anisotropy: Dilley, Texas: 56th Ann. Internat. Mtg., Soc. Explor. Geophys., Expanded Abstracts, 476–479.

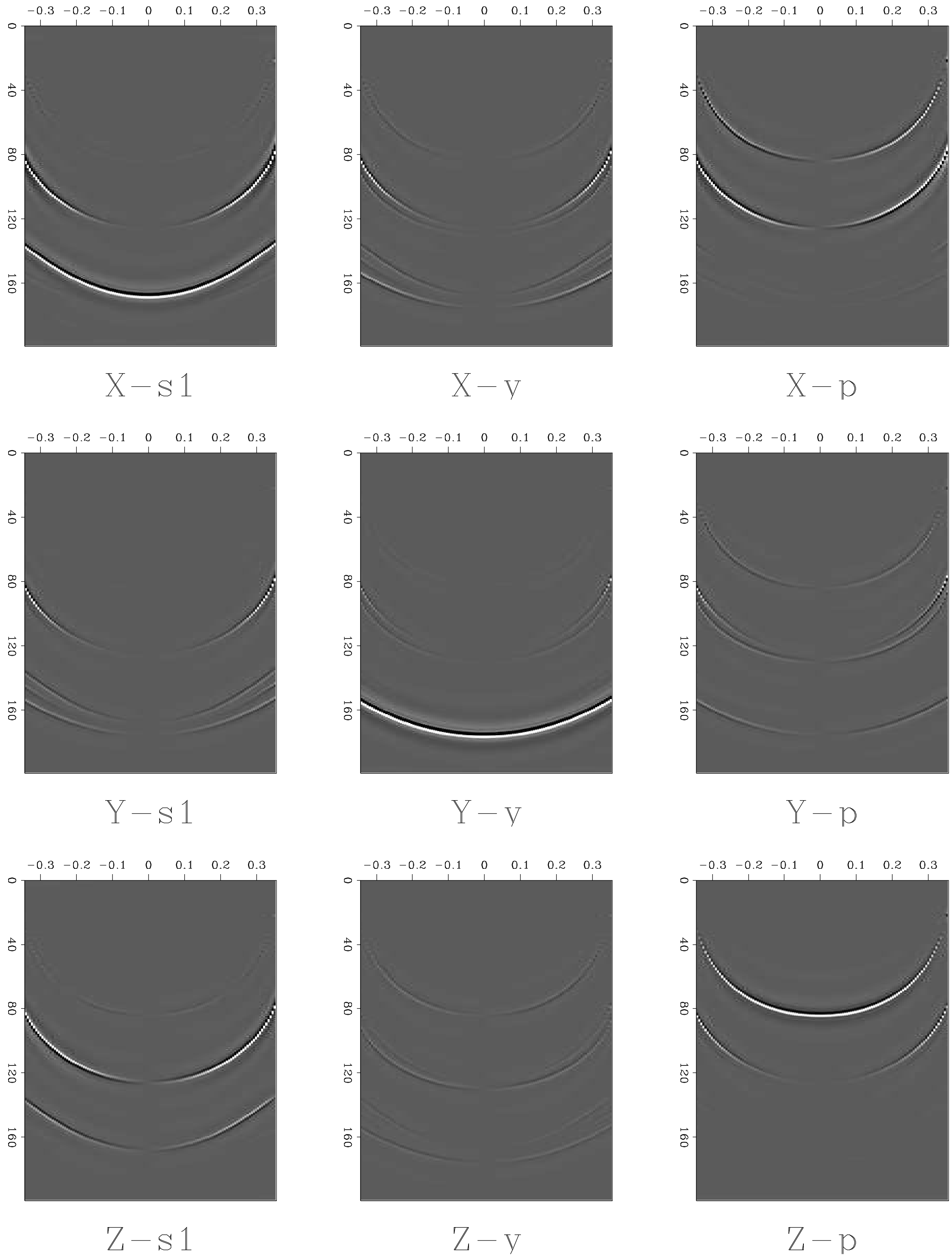

Figure 8: Nine-component gather after application of the receiver P/S_1 operator. The upcoming P waves have been removed from the first column and the upcoming S_1-waves have been removed from the third column. dave-rec-sep [ER]

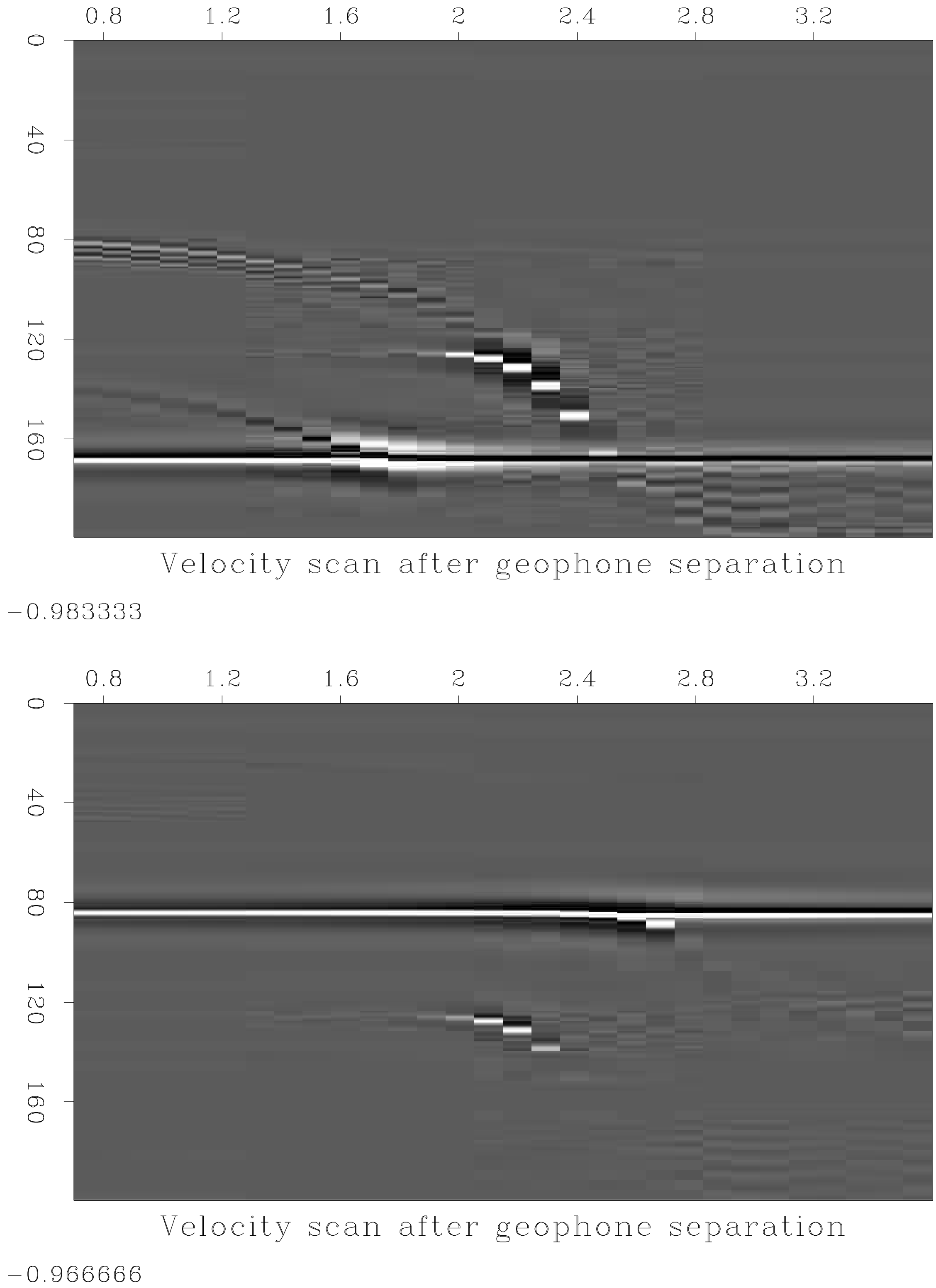

Figure 9: Constant velocity stack panels for the data after receiver P/S_1 separation. The top panel is the X-s_1 component and the bottom panel is the Z-p component. There is little upcoming P-wave energy on the X-s panel and little upcoming S_1-wave energy on the Z-p panel. dave-vel-recsep [ER]

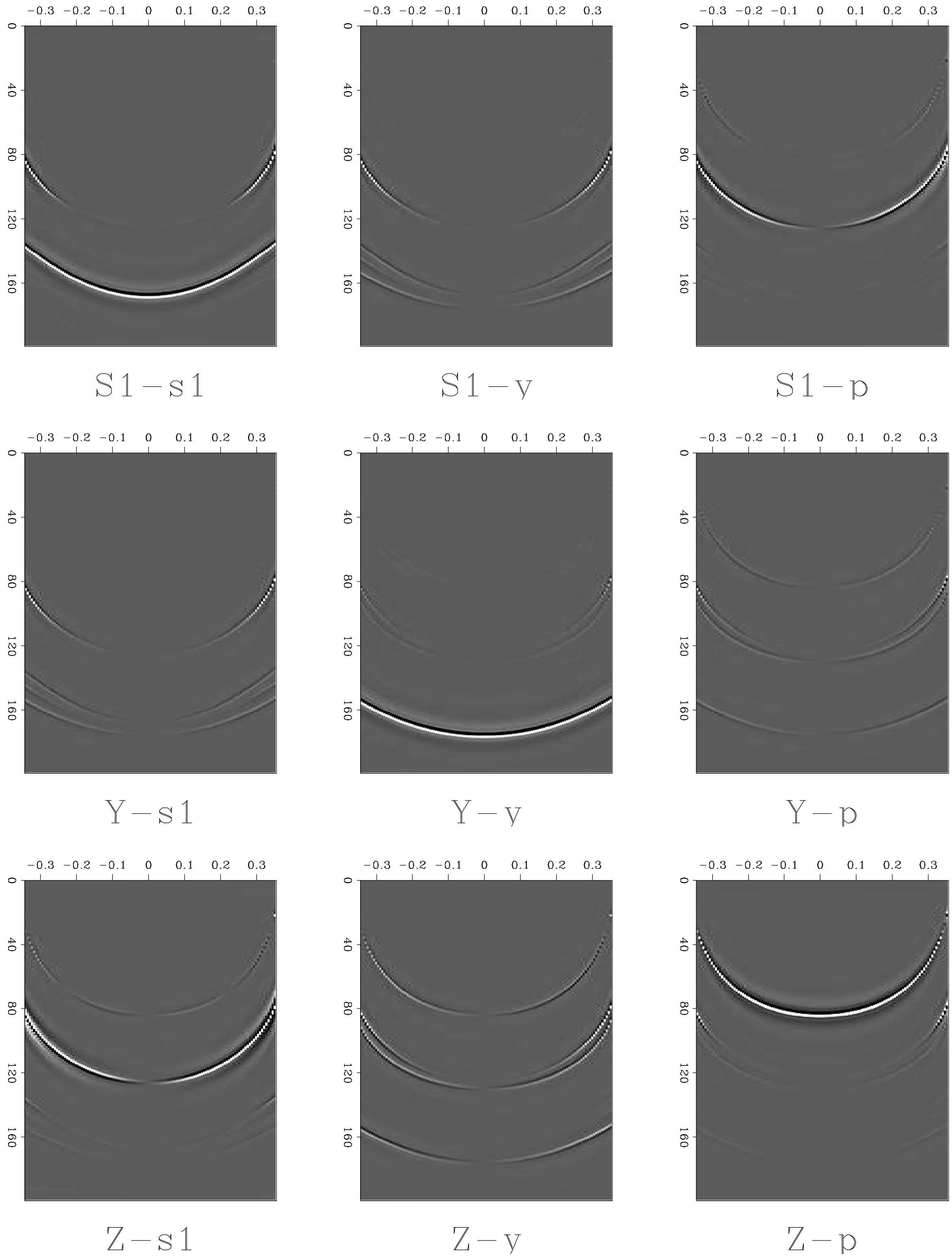

Figure 10: Nine component gather after application of the source and receiver P/S_1 operators. The downgoing P waves have been removed from the first row and the downgoing S_1-waves have been removed from the third row. dave-src-sep [ER]

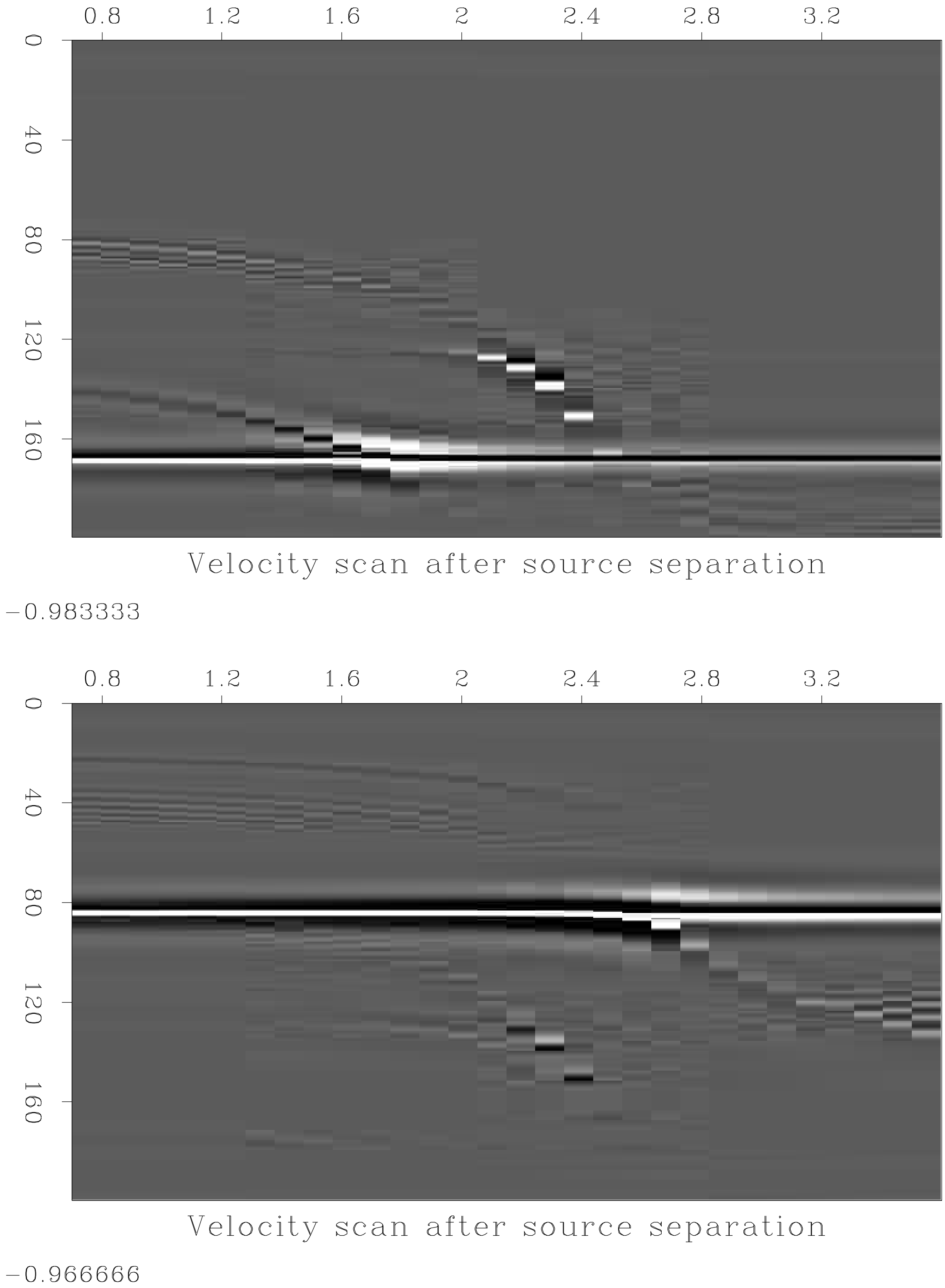

Figure 11: Constant velocity stack panels for the data after source and receiver P/S_1 separation. The top panel is the S_1-s_1 component and the bottom panel is the P-p component. The separation is not complete but most of the unwanted energy has been removed. dave-vel-srcsep [ER]

Herrmann, P., Verschuur, D.J., Wapenaar, C.P.A., and Berkhout, A.J., 1989, Decomposition of multicomponent data into primary P- and S-wave responses: 51st Mtg. of the EAEG, Abstracts of papers, 69–70.

Nichols, D.E., 1989, Converting surface motions to subsurface wavefields: SEP–**61**, 179–200.

Nichols, D.E., 1991, A Simple Modeling Scheme for Layered Anisotropic Media: SEP–**70**, 337–356.